2015 IEEE International Conference on Advanced Intelligent Mechatronics (AIM)
July 7-11, 2015. Busan, Korea

A Novel Propeller–Type Climbing Robot for Vessels Inspection

Mohamed G. Alkalla[a] , Mohamed A. Fanni[b] and Abdelfatah M. Mohamed[c]

Abstract— **This paper is proposing and designing a novel propeller–type climbing robot for exploring the interiors of industrial vessels and enables a human outside it to implement required regular inspection tasks efficiently. There are two main adhesion systems in the literature: magnetic and air suction systems. The magnetic system climbs surfaces made of ferromagnetic materials only, while air suction system can handle neither irregular surfaces due to possible seal damage nor cylindrical surfaces. Opposite to previous climbing robots, the proposed robot here can climb and navigate vessels made from different materials besides handling possible irregular or cylindrical surfaces. Its main task is visual inspection of welds and any critical spots inside these vessels. The novelty of this robot comes from utilizing a hybrid actuation system consists of upturned propellers fixed on mobile robot with motorized wheels. The pressure generated from the upturned propellers increases the friction force between the wheels of the mobile robot and the wall. The wheels' motors generate the required torque either to fix the robot at any position or to move it to any place. Since the motion of the robot comes mainly from the motorized wheel, the stability of the system during navigation is guaranteed. Simulation and control results of the designed robot using ADAMS and Matlab softwares prove the success and feasibility of the robot concept.**

I. INTRODUCTION

The systems which have a capability of climbing vertical structures or navigate inside tanks and vessels have an increasing importance in the last two decades. The application fields of the climbing robots are ranging from welding of ship hulls to the inspection of steel bridge or nuclear power plants. Common systems such as 'Rest' which uses six legs and magnetic pads for climbing [1], are applied for such tasks. It is realized that such climbing systems are mainly adopted in places which cannot be reached by humans, where the direct access for the human is too expensive and dangerous. Almost all climbing robots are depending on two main systems (locomotion and adhesion system) to keep the robot attached to the vertical structures. The climbing robot needs to be designed based on the desired functions and field of applications and these aspects define which locomotion and adhesion principle are needed. There are many locomotion principles such as wheels [2], tracks [3], sliding frames [4], arms and legs [5]. Each locomotion system depends on the nature of the surface which these robots are moving on and each one has an advantage over the others at certain requirements, see [6]. There are many adhesion systems such as magnetic, pneumatic, mechanical, electrostatic and chemical adhesion systems. The last two adhesion systems are less common than the others. The magnetic adhesion system depends on the magnetic force between robot and the vertical structure. It is used only for the ferromagnetic material structures. Some climbing robots make use of this adhesion system such as REST robot [1]. The second common type of adhesion system is a pneumatic system which depends on air suction, and the attraction force between the robot and the wall is proportional to the pressure difference between the pressure chamber or suction cup and the atmosphere. There are a lot of climbing robots make use of this principle such as CROMSCI, which combines an omni-directional drive system with an adhesion system equipped with a seven-chamber adhesion system [7]. This pneumatic adhesion type is used for flat and even surfaces. The third common adhesion system uses mechanical gripers and claws and it is suitable for the rough surfaces, such as RISE robot [8]. Some new but less common approaches for adhesion which arise with the material science are electrostatic principle which generate electrostatic or Van der Waals forces between the surface and the robot, such as STICKYBOT [9] and chemical adhesion which uses thermal glue or sticky tapes as [10]. A simple survey on the common climbing robots is presented in [6].

Mohamed G. Alkalla is Ph. D. Student, Mohamed A. Fanni is Associate Professor and Abdelfatah Mohamed is Professor at Mechatronics and Robotics Engineering Department, School of Innovative Design Engineering, Egypt-Japan University of Science and Technology (E-JUST), New Borg El-Arab, Alexandria, PO Box: 21934, Egypt. $^{(a,b)}$ on leave: Production Eng. and Mechanical Design Dept., Faculty of Engineering, Mansoura University, Egypt. $^{(c)}$ on leave: Electrical Engineering Department, Faculty of Engineering, Assiut University, Egypt. E-mail:{mohamed.gouda, mohamed.fanni, abdelfatah.mohamed}@ejust.edu.eg.

II. THE PROPOSED CLIMBING ROBOT

A novel climbing robot is proposed here which can overcome a lot of difficulties that faced previous climbing robots such as: Is the vessel material ferrous or not? Is the surface even or not? These aspects will not be a problem in this proposed robot design, since it depends on upturned propellers mounted on a mobile robot. This idea is opposite to flying concept. The propellers are supposed to push and generate normal force against the vessel wall. Consequently, it does not need a ferrous structure like magnetic adhesion robots, flat/regular surfaces like suction chambers robots, or rough surfaces for grippers like mechanical adhesion robots. A propellers system is previously used only for driving a climbing robot as presented in [11] and [12]. This system used inclined propellers not only to move the robot forward but also to stick it to the wall during motion, as shown in Fig. 1. Also there was no steering system for this robot where passive wheels are used. So, the robot can't turn left or right. Moreover, the navigation stability was a major problem in this robot, as mentioned in [6]. The proposed idea here is based on a hybrid actuation system which utilizes both

978-1-4673-9107-8/15/$31.00 ©2015 IEEE

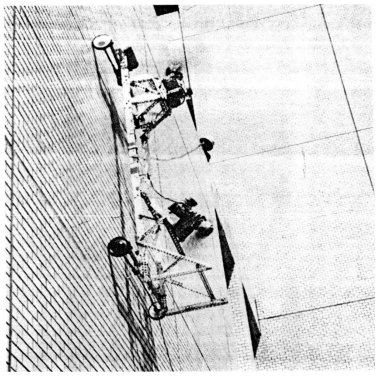

Fig. 1. Propeller-type climbing robot [11].

thrust forces of upturned-propellers and torques of wheels-motors as an adhesion system, while utilizes the motorized wheels as locomotion system. The wheels' motors generate the required torque either to fix the robot at any position or to move it to any place. So, this proposed robot has many advantages over the former one such as the steering capability, fixing the robot at any position and navigation stability for accurate inspection tasks. Since the proposed adhesion mechanism does not depend on a magnetic force or air suction which needs sealing means, it can climb walls made of arbitrary materials and can handle any obstacles that would damage the seals of the air suction robots if they were used. The proposed climbing robot will be introduced here starting with conceptual design that suggest different wheels/propellers arrangements in section III. The detailed mechanical design will follow for the best concept in section IV where the optimum topology of the robot structure as well as proper selection of wheels, propellers and motors are carried out. Dynamic simulation using ADAMS for the proposed system is going to be accomplished in section V. Finally, PI control with gravity compensation is applied to the robot for controlling its velocity in section VI.

III. STRUCTURAL DESIGN OF THE PROPOSED CLIMBING ROBOT

A novel versatile inspection robot for industrial vessels (VIRIV) is going to be designed. Three conceptual designs for the versatile inspection robot are generated. Design 1 uses one propeller, two motorized standard wheels, and two omni-directional wheels placed on opposite axles, as shown in Fig. 2. (left). So the drag-moment of the propeller is overcome by the frictional force acting on the motorized wheels. The advantage of this model is that the robot have only three actuators (one for propeller and two for wheels), but its drawbacks are the difficulties in steering and navigation. Design 2 uses two coaxial propellers (right and left handed) turn in opposite directions. In addition to two driving motorized wheel and two omni-directional wheels. Thus the drag moments generated from the two propellers eliminate each other. The advantages of this design is its mathematical model simplicity and greater normal force against wall compared to design 1, see Fig. 2. (right). Finally, 3^{rd} design is like 2^{nd} design except that it uses four standard

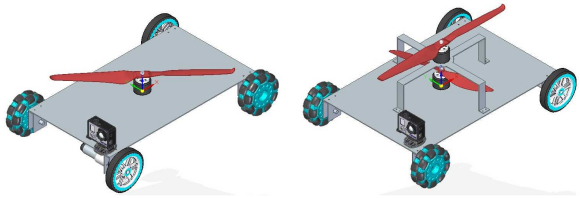

Fig. 2. Left: Design 1, with two motorized, two omni-wheels and one rotor. Right:Design 2, with two motorized wheels, omni-wheels and rotors.

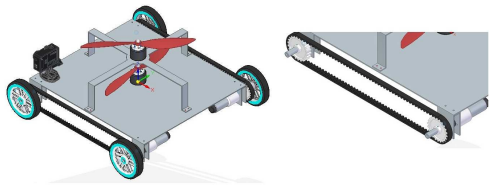

Fig. 3. Design 3, with four motorized wheels, timing belts and two rotors.

wheels and the two right wheels are driven by one motor while the two left wheels are driven by another motor using timing belts, as shown in Fig. 3. The advantages of this design are the same as 2^{nd} design besides the high frictional forces at the the four wheels. Thus, higher wheels traction forces during climbing and holding on the vertical structures are available. The third design is the best one due to its preceding advantages, so the mechanical design is carried out for this design and utilizes the static and dynamic equations. The propellers' normal forces that are exerted on the robot platform, robot's weight, torque applied on each wheel and the coefficient of friction between wheels' tires and climbing surface are taken into consideration. At any position on the wall or inside the vessel, the thrust force exerted from the propeller is always normal to the climbed surface while the weight of the robot is vertically downward. Figure 4 shows all forces acting on the robot chassis and the wheels. N_i and F_{fi} are the normal and frictional forces acting on the wheel i respectively, F_N is the propellers' thrust force acting on robot

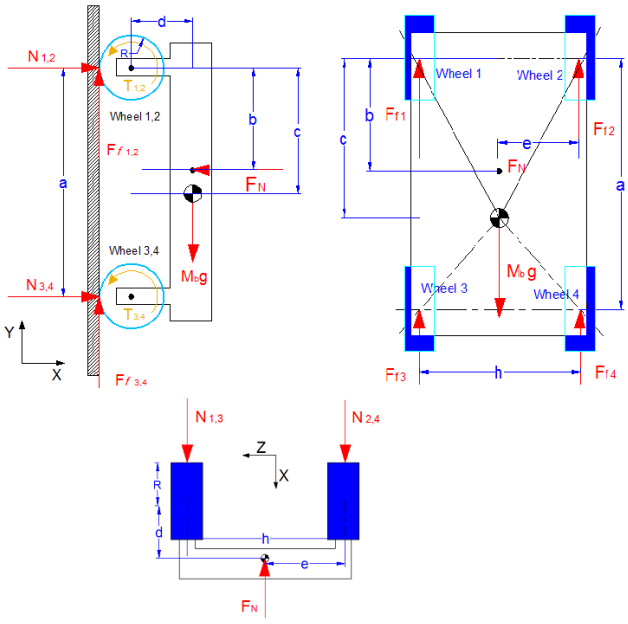

Fig. 4. Free body diagram of the robot chassis and wheels.

chassis, a and h are length and width of the chassis, b is the distance between thrust force F_N and the front wheel axes, c is the distance from chassis centroid to front wheel axes in longitudinal direction, d is normal distance from centroid to a plane contains wheels axes, e is the distance between the centroid and the right wheels in the lateral direction, R is the wheel radius. The static equations which hold the robot on the vertical wall are driven below:

$$N_1 + N_2 + N_3 + N_4 = F_N \tag{1}$$

$$F_{f1} + F_{f2} + F_{f3} + F_{f4} = W \tag{2}$$

$$-(F_{f1} + F_{f3}) \cdot (h - e) + (F_{f2} + F_{f4}) \cdot e = 0 \tag{3}$$

$$(N_1 + N_3) \cdot (h - e) + (N_2 + N_4) \cdot e = 0 \tag{4}$$

$$-(N_1+N_2)\cdot c - W\cdot(R+d) + F_N\cdot(c-b) + (N_3+N_4)\cdot(a-c) = 0 \tag{5}$$

It is found that the torque T_i and the frictional forces at front and rear wheels are equals in each side so,

$$F_{f1} = F_{f3} \tag{6}$$

$$F_{f2} = F_{f4} \tag{7}$$

The model is statistically indeterminate problem thus, the force displacement method for compatibility is used with considering the chassis as a rigid body, thus, the last equation is as follows:

$$N_1/k_{w1} - N_2/k_{w2} - N_3/k_{w3} + N_4/k_{w4} = 0 \tag{8}$$

Where, k_{wi} is the stiffness of wheel i. The frictional force F_{fi} should always be less than the normal force N_i multiplied by the static coefficient of friction μ_s as expressed in (9). This check is essential to validate the design. The relation between the wheels torques and the frictional forces is defined in (10).

$$F_{fi} \leq \mu_s N_i \tag{9}$$

$$T_i = F_{fi} \cdot R \qquad for \quad i = 1, ..., 4 \tag{10}$$

IV. STRUCTURAL OPTIMIZATION

A detailed design is carried out to determine the sizes and specifications of the motors, propellers and wheels as well as type of the material used for chassis. Also structural optimization such as size and topology optimization are applied for the chassis to obtain a minimum weight robot.

A. SIZE OPTIMIZATION BASED ON WEIGHT MINIMIZATION

Size optimization technique is applied to the robot to optimize its weight which is an important issue for such climbing robots. There are many constraints for the optimization such as the rotor thrust force which is limited to 3 kg for each rotor. Also there are the motors whose rated maximum torques are proportional with its sizes and weights. On the other hand there is a relation between maximum frictional force on the wheel and its normal force, as in (9). Thus, it is a complicated optimization problem to be solved. It also depends on continuous values of some parameters such as dimensions of chassis and discrete values of other parameters such as maximum motors torque, maximum rotors' thrust force or propellers diameters. The objective function is minimization of the total robot weight W_T subjected to some constraints as illustrated above in (11) to (20) and all these constraints should satisfy equations (1) to (8).

$$\min_x : W_T = (a \times h \times t)\rho g + W_a \tag{11}$$

$$s.t. : F_{fi} \leq \mu_s N_i \tag{12}$$

$$F_N \geq W_T/\mu_s \tag{13}$$

$$T_1 + T_3 \leq T_{max} \tag{14}$$

$$T_2 + T_4 \leq T_{max} \tag{15}$$

$$a, h \geq D_p \tag{16}$$

$$D_p/2 \leq b \leq a - D_p/2 \tag{17}$$

$$N_i \geq 0 \tag{18}$$

$$\delta \leq \delta_{max} \tag{19}$$

$$\sigma \leq S_y/F_s \tag{20}$$

W_a is a payload weight consists of all components of the robot except the chassis weight such as (motors, wheels, rotors, propellers, controllers, pulleys, belts and camera). t, ρ are thickness and density of the chassis respectively. T_{max} is the maximum torque applied by each motor and D_p is propeller diameter. δ, δ_{max} are the deflection of the chassis and maximum allowable deflection respectively. σ, S_y and F_s are the maximum stress of chassis, yielding strength of chassis material and factor of safety respectively. The design variables are a, h, b, d and R. The initial design parameters are shown in TABLE I, where F_N is taken according to the maximum allowable thrust force generated by the two rotors which is 5 kg at the normal load current. The smallest propeller diameter which is suitable for the selected rotor and generate the required thrust load is 12".

An interface between Matlab and ANSYS softwares is established to accomplish the optimization process. Matlab optimization toolbox is utilized to carry out the optimization task while, finite element analysis using ANSYS is utilized to calculate deflection and stress. The lower bound values for a, h and b are D_p, D_p and D_p/2 respectively to make sure that the propellers are within the robot boundary for

TABLE I
INITIAL DESIGN PARAMETERS FOR SIZE OPTIMIZATION (ALUMINUM 6061–T6 WITH 2 mm THICKNESS)

Initial Design Parameters	Values
Payload weight W_a	1 kg
Rotors thrust load F_N	5 kg
Density ρ	2700 kg/m^3
Coefficient of static friction μ_s	0.4
Max. motor torque T_{max}	0.5 $N.m$
Propeller diameter D_p	12" or 0.31 m
Max. allowable deflection δ_{max}	3 mm
Yielding strength S_y	105 Mpa
Modulus of elasticity E	70 Gpa
Factor of safety F_s	1.5
Initial chassis size $(a \times h)$	$0.40 \times 0.40m$

TABLE II

FINAL RESULTS OF THE ROBOT CHASSIS SIZE OPTIMIZATION

Optimum Parameters	Values
a, h, b, d, R	0.35, 0.35, 0.175, 0.02, 0.05 m
Maximum stress	58.331 Mpa
Deflection	1.9 mm
Normal force N_1 = N_2	11.095 N
Normal force N_3 = N_4	13.422 N
Friction force $F_{f1,2,..,4}$	4.0736 N

safety. The lower bound values for d and R are 0.02 and 0.05 m for a reasonable gap between robot and climbed surface to overcome obstacles and to assemble the wheels' motors easily. While the upper values are 0.6, 0.6, 0.6-D_p/2, 0.1 and 0.1 m due to size limitation of the vessel entrance. The optimization process results in an optimum chassis size of 0.35 $\times$ 0.35 m and a total robot weight of 1.661 kg while the initial design was 1.864 kg, also the final deflection is 1.9 mm which is less than the initial value. The final results are shown in TABLE II.

B. TOPOLOGY OPTIMIZATION BASED ON COMPLIANCE MINIMIZATION

Topology optimization technique is used for optimizing the robot chassis and minimizing its compliance. Continuous relative densities of all elements inside the design domain are used as the design variables. The topology optimization is mainly based on relocating the material within the model to make it solid or void and create a model with various shapes and sizes. The density and modulus of elasticity of the elements are expressed as follow:

$$\rho_i(x_i) = \rho_0 x_i, \quad E_i(x_i) = E_0 x_i^p \tag{21}$$

$$0 < x_i \leq 1 \tag{22}$$

Where, x_i, ρ_i and E_i are the continuous relative density, element density and modulus of elasticity respectively. ρ_0 and E_0 are the initial density and elasticity of the base material. p is a penalization power to penalize the intermediate densities. Topology optimization is accomplished using the method of moving asymptotes (MMA) inspired by Svanberg in [13] using MATLAB. This optimization problem is based on compliance minimization as illustrated in (23) to (26).

$$\min_x : C(\mathbf{x}) = U^T K U = \sum_{i=1}^{n} (x_i)^p u_i^T k_i u_i \tag{23}$$

$$s.t. : V(\mathbf{x})/V_0 = V_{frac} \tag{24}$$

$$KU = F \tag{25}$$

$$0 < x_{min} \leq x_i \leq 1 \tag{26}$$

where, U and F are the global displacement and force vectors, respectively; K is the global stiffness matrix, u_i and k_i are the element displacement vector and stiffness matrix, respectively. $V(\mathbf{x})$ and V_0 are the material volume and the initial volume respectively; where V_{frac} is the prescribed volume fraction. For more details on topology optimization technique, see [14]. The initial design model with boundary conditions and loads is shown in Fig. 5, while the optimum

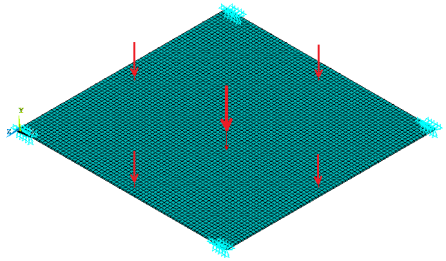

Fig. 5. Initial design of robot chassis with boundary conditions and loads modeled by ANSYS.

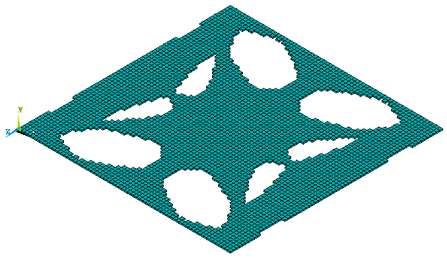

Fig. 6. Final Topological optimum design of VIRIV robot chassis.

topological design of the robot chassis is shown in Fig. 6. The final results for topology optimization is shown in TABLE III at initial design variables $\mathbf{x_0}$ and volume fraction equals 0.65. Carbon fiber can be used as alternative robot chassis material. The final topological deign is modeled using Solid Edge ST6 software and also a finite element analysis is applied to check the strength and rigidity of the robot chassis, as shown in Fig. 7

TABLE III

RESULTS OF ROBOT CHASSIS TOPOLOGY OPTIMIZATION

Properties	**Compliance** ($N.m$)	**Max. Defl.** (mm)	**Max. Stress** (Mpa)
Initial Design	0.278845	2.9691	58.3314
Topological Design	0.113703	2.6615	67.7983

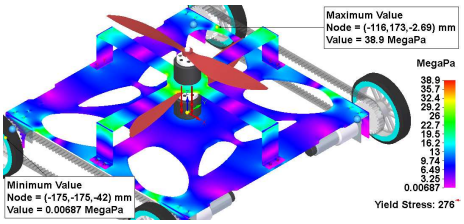

Fig. 7. FEA using Solid Edge for VIRIV Robot chassis.

V. ADAMS RESULTS

Dynamic simulation of the climbing robot is applied using MSC ADAMS software. Rotors thrust load of 5 kg is used. Each wheel is actuated with a torque equals to 203.7 $N.mm$. The whole robot weight is 1.661 kg as indicated previously. ADAMS contact facility is used to model the contact between the robot wheels and the climbed surface. The parameters of the contact are as follow: The static and dynamic coefficient of friction are equal to 0.4 and 0.3 respectively, the stiffness of the wheels is 10^5 N/mm and the damping coefficient is 10^4 $N.s/mm$. Also the stiction transition velocity and the friction transition velocity are 0.1 mm/s and 100 mm/s. The climbing robot model is tested on both a vertical wall and inside a vessel with a diameter of 5 m.

A. VERTICAL MODEL

The climbing robot model is tested using ADAMS at the specified torque of 203.7 $N.mm$ and thrust force of 49.05 N which specified above for holding the robot on the wall at certain location. It is found that the robot remains at its position without any movement. When the wheels' torques increase a little bit to become 206 $N.mm$, the robot begins to climb the wall and goes upward in the vertical direction (y-direction), as shown in Fig. 8. This figure shows the position and linear velocity of the robot in the vertical direction versus time.

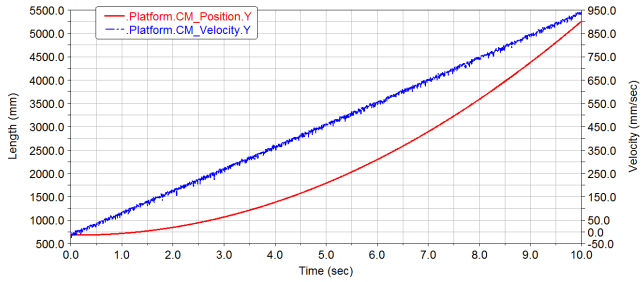

Fig. 8. The vertical position and linear velocity of the platform in y-direction versus time.

B. VESSEL MODEL

The second test is make the robot climb the inner cylindrical surface of a vessel of 5 m diameter , as shown in Fig. 9. It is found that at the same thrust force 49.05 N, the torque on each wheel can decrease to 180 $N.mm$ and still climb the interior surface of vessel. The motion of the

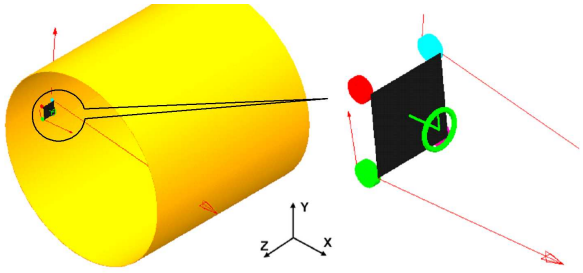

Fig. 9. Modelling and simulation of the climbing robot inside vessel using ADAMS.

robot begins from the vessel's bottom and then moves on the inner cylindrical surface to climb the vessel and reaches the maximum vertical position on the vessel's ceiling at a time nearly equal to 2.5 sec and goes down again in a circular path. The position in x, y directions and the linear velocity magnitude of the robot are shown in Fig. 10

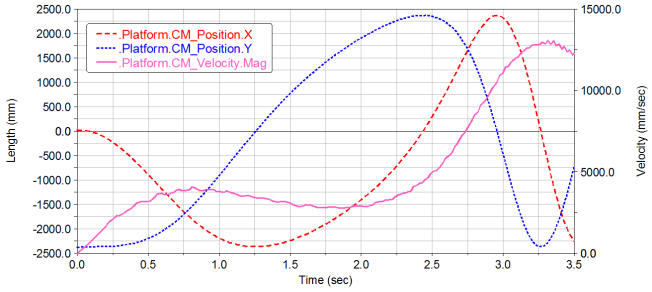

Fig. 10. Robot chassis position in x and y directions and linear velocity magnitude of robot versus time.

VI. CLIMBING ROBOT CONTROL

PI control is applied to the proposed climbing robot. Firstly, it has been implemented to climb a vertical wall with constant speed, where the robot in the previous section has an undesirably increasing speed. So the climbing robot was controlled to climb the vertical wall with moderate speed equal to 0.2 m/s to facilitate and improve the inspection process. In order to utilize both dynamic simulation capability of ADAMS and control facilities of Matlab/Simulink, an interface between the two software is established, as shown in Fig. 11. The inputs to the ADAMS model are the torques

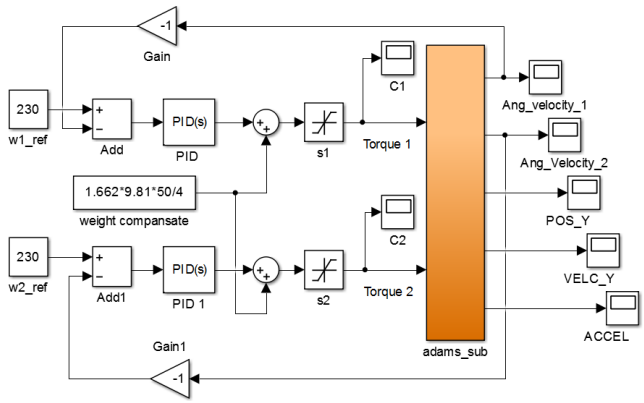

Fig. 11. Matlab/Simulink/ADAMS model for vertical wall climbing robot.

applied to the left and right wheels, where the two wheels in each side have the same torque. The outputs of the model are the angular velocities of the right and left wheels, the vertical position in y-direction, the linear velocity and acceleration of the robot in y-direction. The angular velocities of the wheels is controlled to a certain value equal to 230 deg/s (4.014 rad/s) which equivalent to a linear velocity of 0.2 m/s. The angular velocities are used as feedback signals to the PI controller where, they can be measured easily by the DC geared motors encoders. The response of the system becomes faster by adding a constant term to the input torques of the wheels to compensate the robot weight. The gains of the PI controller are tunned to get the velocity response fast and without any overshoot. The proportional gain k_P and the integral gain k_I are found to be 1.3 and 0.02 respectively. The vertical position obtained from the controlled system is shown in Fig. 12. The linear velocity of the robot is shown in Fig. 13, it shows that the response of the velocity is smooth

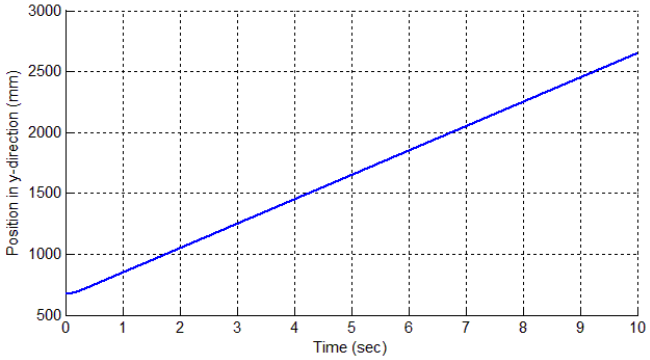

Fig. 12. Position in y-direction of the robot with PI control.

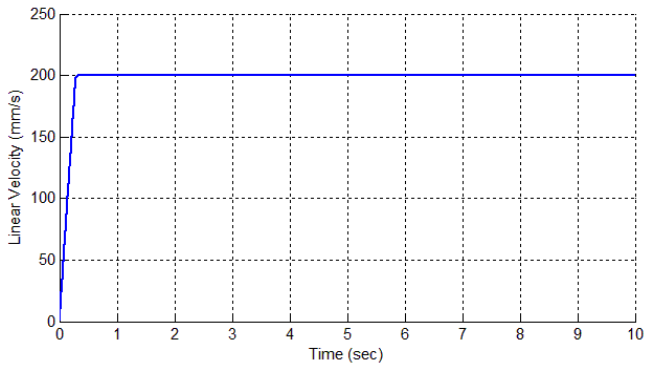

Fig. 13. Linear velocity in y-direction of the robot with PI control.

without overshoot and the settling time is equal to 0.271 sec. Sometimes, the inspection robot is required to stop at a certain position to take images or do a specific job. To check the robot ability to do that, the controller is adopted to climb the wall and stop after 5 sec. The position and linear velocity of the robot in this case, are shown in Fig. 14 and Fig. 15. The robot stops at position of 1.6 m. So, these results prove the navigation stability of the system.

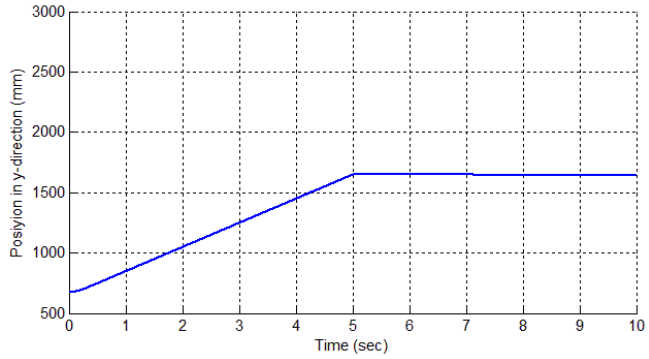

Fig. 14. Position in y-direction with PI control, the robot stop at 5 sec.

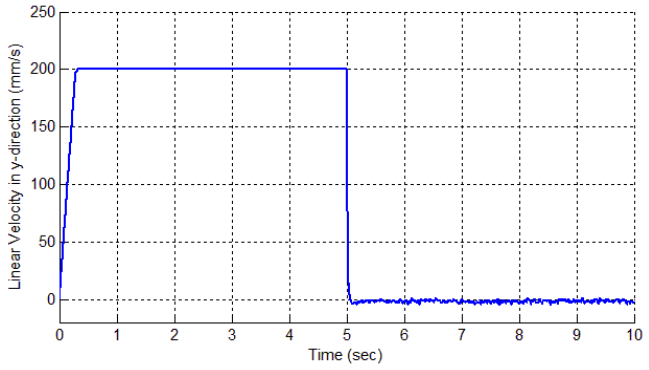

Fig. 15. Linear velocity in y-direction with PI control, the robot stop at 5 sec.

VII. CONCLUSIONS

The paper presents a new kind of climbing robot which can inspect petrochemical tanks and vessels without any restrictions on the climbing surface material or obstacles inside them. The new concept of climbing by a hybrid system, which consists of propellers and motorized wheels, is approved using MSC ADAMS software. Both size and topology optimization are applied to obtain a light weight robot. The stability of the overall system during navigation is guaranteed by using such hybrid system. The linear velocity of the robot during climbing the vertical structure is controlled for completing the inspection task efficiently. The motion control of the robot inside the vessel will be accomplished in the future work.

ACKNOWLEDGMENT

The first author is supported by a scholarship from the Mission Department, Ministry of Higher Education (MOHE), The Government of Egypt which is gratefully acknowledged. Professor Krister Svanberg, from the Royal Institute of Technology, Stockholm, is Gratitude thanked for providing us with the method of moving asymptotes code.

REFERENCES

[1] J. Grieco, M. Prieto, M. Armada, and P. de Santos, "A six-legged climbing robot for high payloads," in *Control Applications, 1998. Proceedings of the 1998 IEEE International Conference on*, vol. 1, Sep 1998, pp. 446–450 vol.1.

[2] B. Bridge, J. Shang, B. Bridge, T. Sattar, S. Mondal, and A. Brenner, "Development of a climbing robot for inspection of long weld lines," *Industrial Robot: An International Journal*, vol. 35, no. 3, pp. 217–223, 2008.

[3] W. Shen, J. Gu, and Y. Shen, "Permanent magnetic system design for the wall-climbing robot," in *Mechatronics and Automation, 2005 IEEE International Conference*, vol. 4, July 2005, pp. 2078–2083 Vol. 4.

[4] V. GRADETSKY and M. KNYAZKOV, "Multi-functional wall climbing robot," in *Adaptive Mobile Robotics,Proceedings of the 15th International Conference on Climbing and Walking Robots, CLAWAR, Baltimore, USA, 2012*, pp. 807–812.

[5] S. Kim, M. Spenko, S. Trujillo, B. Heyneman, V. Mattoli, and M. Cutkosky, "Whole body adhesion: hierarchical, directional and distributed control of adhesive forces for a climbing robot," in *Robotics and Automation, 2007 IEEE International Conference on*, April 2007, pp. 1268–1273.

[6] D. Schmidt and K. Berns, "Climbing robots for maintenance and inspections of vertical structures–a survey of design aspects and technologies," *Robot. Auton. Syst.*, vol. 61, no. 12, pp. 1288–1305, Dec. 2013.

[7] D. Schmidt, C. Hillenbrand, and K. Berns, "Omnidirectional locomotion and traction control of the wheel-driven, wall-climbing robot, cromsci," *Robotica Journal*, vol. 29, no. 7, pp. 991–1003, 2011.

[8] M. J. Spenko, G. C. Haynes, J. A. Saunders, M. R. Cutkosky, A. A. Rizzi, R. J. Full, and D. E. Koditschek, "Biologically inspired climbing with a hexapedal robot," *J. Field Robot.*, vol. 25, no. 4-5, pp. 223–242, Apr. 2008.

[9] S. Kim, M. Spenko, S. Trujillo, B. Heyneman, V. Mattoli, and M. Cutkosky, "Whole body adhesion: hierarchical, directional and distributed control of adhesive forces for a climbing robot," in *Robotics and Automation, 2007 IEEE International Conference on*, April 2007, pp. 1268–1273.

[10] K. Daltorio, A. D. Horchler, S. Gorb, R. E. Ritzmann, and R. Quinn, "A small wall-walking robot with compliant, adhesive feet," in *Intelligent Robots and Systems, 2005. (IROS 2005). 2005 IEEE/RSJ International Conference on*, Aug 2005, pp. 3648–3653.

[11] A. Nishi and H. Miyagi, "Propeller type wall-climbing robot for inspection use," *Proc. 10th Int. Symp, on Automation and Robotics in Construction (ISARC)*, pp. 189–196, 1993.

[12] A. Nishi, H. Miyagi, and K. Ishihara, "Development of wall inspection robots," *Proc. 12th Int. Symp, on Automation and Robotics in Construction (ISARC)*, pp. 103–108, 1995.

[13] K. Svanberg, "The method of moving asymptotesa new method for structural optimization," *International Journal for Numerical Methods in Engineering*, vol. 24, no. 2, pp. 359–373, 1987.

[14] M. P. Bendsoe and O. Sigmund, "Topology optimization – theory, methods and applications, handbook." Springer-Verlag Berlin Heidelberg, 2003, pp. 1–13.